^{13}C$(e, p_{0,1})^{12}$B differential cross section

D. Zubanov and M. N. Thompson

School of Physics, University of Melbourne, Parkville 3052, Victoria, Australia

J. W. Jury

Department of Physics, Trent University, Peterborough, Ontario, Canada K9J 7B8

K. Shoda

Laboratory of Nuclear Science, Tohoku University, Mikamine, Sendai 982, Japan
(Received 20 July 1993)

The differential cross sections for the reactions ^{13}C(γ, p_0) and ^{13}C(γ, p_1) have been measured in the energy range 21–26 MeV. Analysis of the present data and the ^{13}C(γ, p) cross section reveals decay of the giant dipole resonance at 23 MeV, via the p_4 channel. The valence neutron does not appear to interact strongly with the ^{12}C core. Isospin splitting effects are observed.

I. INTRODUCTION

A program of measurements of the photoproton and photoneutron cross sections of light nuclei with one or two neutrons outside a closed or semiclosed shell has been carried out over the past few years. The aim was to determine the effect of the valence nucleons on the cross sections and thus to determine the effects on the dipole state configurations. A complete bibliography of the measurements in the series can be found in the review by McNeill et al. [1].

The nucleus ^{13}C is an excellent case in point, and measurements of the ^{13}C(γ, n) reaction cross section [2] and the ^{13}C(γ, p) reaction cross section [3] have studied the resulting pygmy resonance and clarified the resultant isospin effects. In this paper we report the measurement of the proton-energy spectra following the ^{13}C(e, p) reaction at a few angles and the derived partial (γ, p_0) and (γ, p_1) cross sections and angular distributions in the giant dipole resonance (GDR) region. The results provide more detailed information on the configurational nature of the intermediate structures reported in the ^{13}C(γ, p) cross section of Ref. [3] and help to define the role of the valence neutron on core-excited GDR states.

II. EXPERIMENTAL DETAILS

This experiment was performed using the 300-MeV linac and proton spectrometer at the Laboratory of Nuclear Science at Tohoku University. A brief outline of the experimental arrangement is given below; further details are available elsewhere [4].

Electrons were extracted after the first section of the linac and momentum analyzed to produce a beam with energy in the range 21–26 MeV and a momentum spread of 1%. This beam of typically 10–25 μA was focused onto the target by a series of steering coils and quadrupole magnets. The position, size, and shape of the beam spot at the target position were adjusted before each run by remotely viewing the fluorescence from a BeO disk which was mounted on a motorized target frame inside the scattering chamber. The beam spot was approximately circular and typically 1 cm in diameter.

The incident electron flux was measured using a ferrite core monitor located 60 cm before the target. The monitor was calibrated on three occasions during the experiment by passing a known current through it under conditions similar to those in the experiment.

The proton detection system consisted of a Browne-Buechner-type broad-range spectrometer [5] and a ladder of 100 Si(Li) solid-state detectors arranged on the focal plane. The angular range of the spectrometer is from 30° to 140°. The detectors were shielded by 8 cm of lead, 23 cm of iron, and 30 cm of paraffin. A thin aluminized Mylar curtain was placed in front of the detector array in order to discriminate against alpha particles, deuterons, and tritons by decreasing their energy relative to that of protons. Ryan [6] tested the efficiency of this procedure.

Signals from each of the Si(Li) detectors were amplified by an independent preamplifier and amplifier system, and fed through a linear gate, set in coincidence with the beam burst. To reduce background the gate was held open for 15 μs only. A discriminator level was set on signals from each detector to reject noise signals, and the counts above this level were stored as one channel in a 100-channel spectrum covering the proton energy range $0.47E_0 – 1.17E_0$.

The 7.30-mg/cm^2-thick ^{13}C target (98.9% pure) was supported on a thin (9.63-mg/cm^2) tantalum foil and was prepared by mixing 5% by mass of trinitrocellulose binder with the ^{13}C powder. The mixture was diluted with ethyl acetate, and distributed over a circular area 2.75 cm in diameter, using a brush. A background target was prepared by depositing an equal mass of binder over the same area on another tantalum foil of the same thickness.

Targets were mounted in the scattering chamber on a remotely controlled holder. Throughout the experiment

the targets were inclined at 45° to the incident beam direction, with the ^{13}C facing the entrance slit of the spectrometer.

To minimize heating of targets, the beam current was kept below 25 μA. Both visual inspection and weighing of targets after the experiment revealed some mass loss of binder; a greater loss occurred in the background target. The absence of ^{13}C powder in a crucible placed directly below the target confirmed that the small loss in the ^{13}C target mass could be attributed to loss of the binder. The difference in binder mass in the background and foreground targets was accounted for during the analysis stage.

Proton spectra were recorded at 90° for incident electron energies ranging from 21 to 26 MeV in steps of 0.5 MeV. At electron energies of 21.0, 21.5, 22, and 23 MeV, spectra were recorded at angles of 35°, 62.5°, and 115°, and at electron energies of 24, 25, and 26 MeV, data were taken for spectrometer angles of 35° and 140°. In order to record protons with energies between 2.2 and 8.4 MeV it was necessary to use three different spectrometer-magnet settings; one or two settings were used at each electron energy. For each setting of the spectrometer, a spectrum from a Ni target was taken to permit correction for individual channel efficiencies.

With few exceptions, spectra from the background target were taken to complement those obtained from the ^{13}C target. These were usually measured, in turn, under the same beam-tuning conditions.

III. ANALYSIS AND RESULTS

Data collected at each electron energy were reduced, in a consistent manner, to a 100-channel proton-energy spectrum and the background contribution reliably removed.

The background-subtracted proton yields at 90° are shown in Fig. 1. The strength to the ground state of ^{12}B is clearly observed, as is that to the first excited state, which is seen 0.95 MeV from the tip of each spectrum.

A. Derivation
of the ^{13}C(γ, p_0) and ^{13}C(γ, p_1) cross sections

Because the first excited state in ^{12}B is at 0.95 MeV, the region of the ^{13}C(γ, p) proton spectrum between E_x-0.95 MeV and E_x consists entirely of protons emitted to the ground state of ^{12}B. The ^{13}C(γ, p_0) cross section can be deduced from this top 0.95-MeV region of each proton spectrum by dividing by the incident photon spectrum.

Similarly, since the second excited state of ^{12}B is a 1.67 MeV, the region $E_x = 1.67$ to $E_e = 0.95$ MeV consists of protons emitted to both the ground and first excited states. Since the ^{13}C(γ, p_0) cross section can be derived as above, the p_0 contribution can be removed and the ^{13}C(γ, p_1) cross section can be obtained in a similar way to that describe above.

This procedure may, in principle, be applied indefinitely to derive ^{13}C(γ, p_2), ^{13}C(γ, p_3), etc., cross sections.
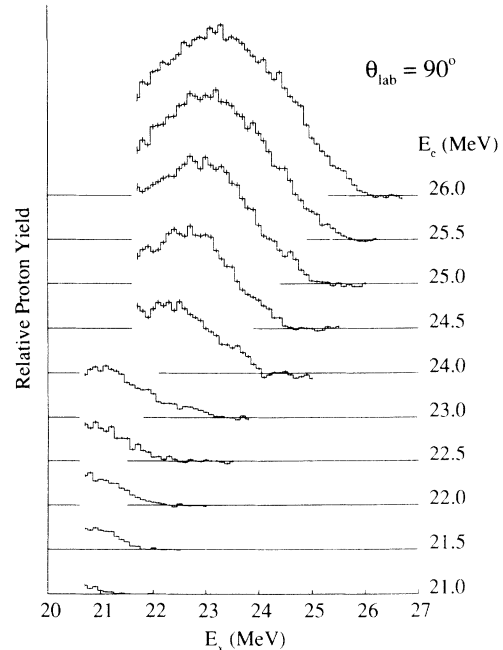

FIG. 1. Background-subtracted proton yields of ^{13}C measured at $\theta = 90°$. The yield is plotted as a function of excitation in the ^{13}C nucleus, E_x, for the different incident electron energies E_e.

In practice, however, the uncertainties progressively increase due to the cumulative errors in subtracting contributions from the lower-lying states.

The resolution of the data shown in Fig. 1 is ~ 830 keV at 22 MeV and ~ 590 keV at 25 MeV, and is due mainly to the proton-energy loss in the target and the momentum acceptance of the incident electron beam. The energy scale shown in Fig. 1 assumes that protons are emitted from the middle of the sample. This assumption leads to an overcorrection for the energy loss for protons emitted from the side of the sample nearer to the detectors and an undercorrection for protons emitted from the far side of the sample. One consequence of this is that for any bin in the proton spectrum, protons are lost to adjacent bins. To a large extent, this loss is compensated by protons transferred in from these channels. However, this cancellation is not complete, especially because the derivation of the cross section as described below uses the top section of the spectrum, where the virtual photon spectrum is changing rapidly.

Allowance for this was made by folding into the virtual photon spectrum, a rectangular resolution function with a width corresponding to the proton energy loss in the full thickness of the target. Without this correction, the derived cross section would be systematically lower by about 8%.

The photon spectrum used in this unfolding process was composed of contributions from both the virtual and real bremsstrahlung spectra. Although the dominant component was the virtual photon spectrum, there was a contribution of real bremsstrahlung produced by electrons incident on both the titanium entrance window to
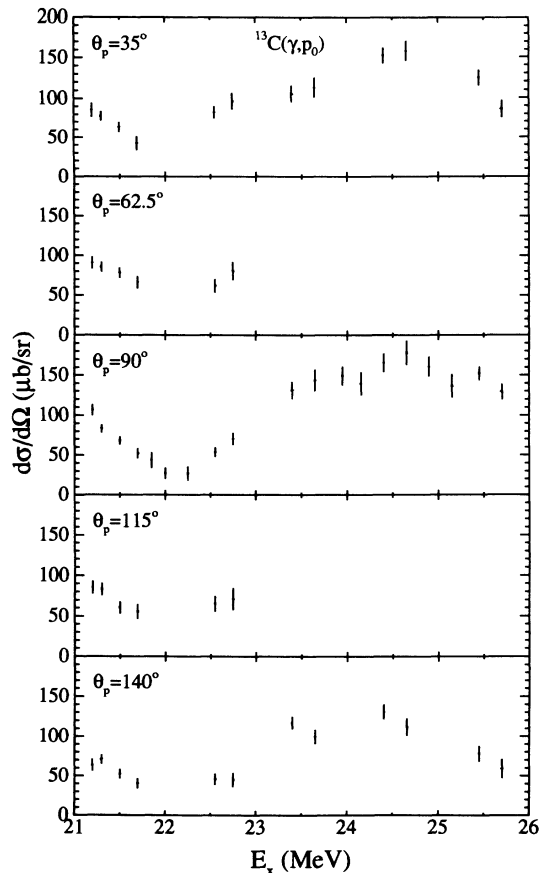
FIG. 2. Differential cross sections for the ^{13}C$(\gamma,p_0)^{12}$B reaction.

the scattering chamber and the tantalum backing of the target. The components were therefore calculated from the $E1$ virtual photon spectrum of Barber and Wielding [7] corrected for Coulomb distortion [8], and the Schiff integrated-over-angles spectrum [9].

In deriving the partial cross sections, the proton yield 300 keV from the p_0 cutoff was rejected from the analy-
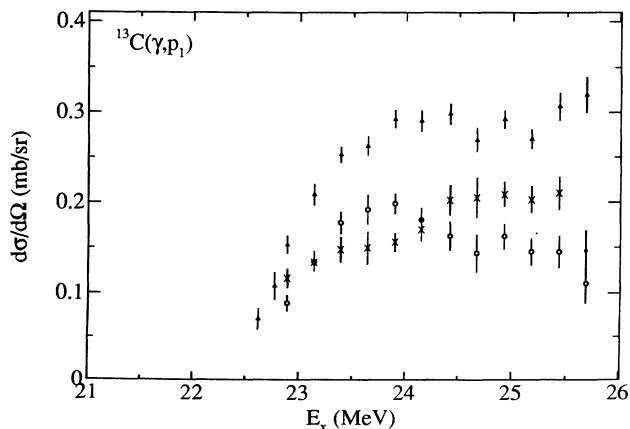

FIG. 3. Differential cross sections for the ^{13}C$(\gamma,p_1)^{12}$B reaction at $\theta_{lab} = 35°$ (crosses), 90° (triangles), and 140° (circles).

sis of all spectra. The large uncertainties near the tip of both the photon spectrum and the proton yield rendered this region unreliable. The smearing of the p_1 proton group into the p_0 region limited the useful bin size for the derivation of the ^{13}C(γ,p_0) cross section to 300 keV for $E_\gamma < 23.5$ MeV and to 400–500 keV for $E_\gamma > 23.5$ MeV. In the derivation of the ^{13}C(γ,p_1) cross section, a 700-keV-wide bin was used for $E_\gamma > 23.5$ MeV since there was no evidence from the difference spectra of significant population to the second excited state in ^{12}B. The midpoint of each energy bin was assigned as the excitation energy of the derived cross section.

The ^{13}C(γ,p_0) and ^{13}C(γ,p_1) differential cross sections at the measured angles are shown in Figs. 2 and 3, respectively.

IV. DISCUSSION

A. Comparison with the ^{13}C(γ,p) cross section

Despite the incomplete data set, as evident from the figures, it was possible to fit the angular distribution with the standard Legendre polynomial expansion

$$\frac{d\sigma}{d\Omega} = A_0(E)\left[1 + \sum_{i=1}^{i=n} a_i(E)P_i(\cos\theta)\right].$$

In the energy region below 23 MeV, where data at five angles were available, the ^{13}C(γ,p_0) cross section was fitted to provide the coefficients A_0, a_1, and a_2. These are shown in Fig. 4. Above 23 MeV, where measurements were taken at only three angles, fits to the data assuming a pure $E1$-type dependence of the form $a + bP_2(\cos\theta)$, gave a large reduced χ^2, indicating the need to include the P_1 term in the fit. Since a χ^2 fit to order 3 for three data points is not possible, exact coefficients were therefore extracted.

The integrated-over-angles cross sections for the ^{13}C(γ,p_0) and ^{13}C(γ,p_1) cross sections were determined from smooth curves drawn through the A_0 coefficients. This provided a basis for comparison with the total ^{13}C(γ,p) cross section measured by the activation-yield-curve method reported by Zubanov et al. [3] and by Dennisov, Kulikov, and Kul'chitskii [10]. The overall uncertainty in the ^{13}C(γ,p_0) and ^{13}C(γ,p_1) cross sections and their sum is estimated to be ±15%, with the major uncertainties canceling in the ratio $\sigma(\gamma,p_0)/\sigma(\gamma,p_1)$.

The ^{13}C(γ,p_0) and ^{13}C(γ,p_1) integrated-over-angles cross sections and their sum are shown in Fig. 5, together with the ^{13}C(γ,p) cross sections of Ref. [3] and that reported by Dennisov, Kulikov, and Kul'chitskii [10]; the latter data set has been translated up in energy by 400 keV. The results of Patrick et al. [11] do not provide any structure information, but are included to confirm the overall shape and magnitude of the (γ,p_0) and (γ,p_1) cross sections.

Experimental limitations did not allow the ^{13}C(γ,p_0) cross section to be determined over the resonance at 20.7 MeV, but just above this resonance, in the valley before
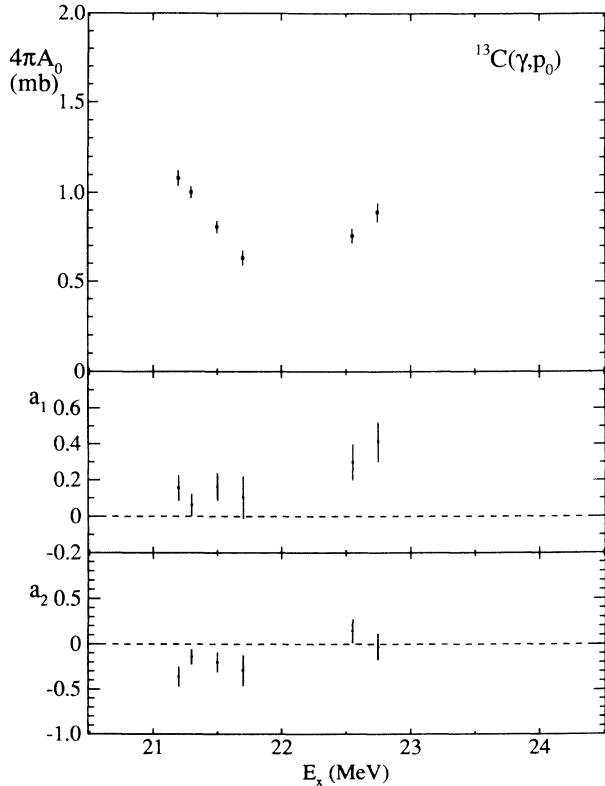
FIG. 4. Integrated-over-angles cross section $(4\pi A_0)$ and the angular distribution coefficients (a_0 and a_1) as a function of excitation energy for the $^{13}C(\gamma, p_0)$ reaction.

the main GDR, it is clear that the $^{13}C(\gamma, p_0)$ cross section dominates. The ratio $\sigma(\gamma, p_0)/\sigma(\gamma, p)$ in this energy region is 0.85±0.20, indicating that within the experimental uncertainites the $^{13}C(\gamma, p_1)$ cross section constitutes about 15% of the total cross section. Reliable determination of the $^{13}C(\gamma, p_1)$ cross section below 22.5 MeV could
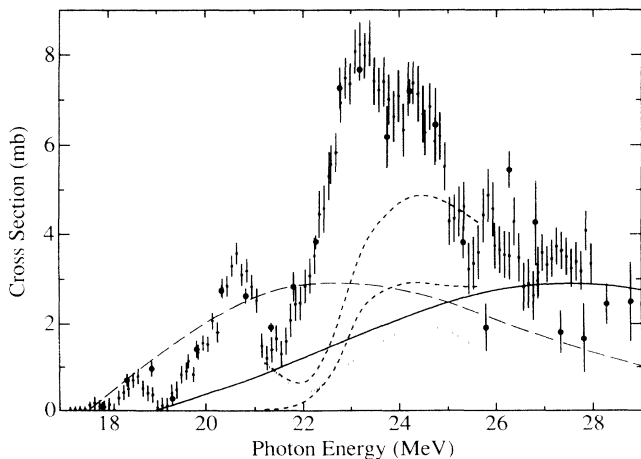

FIG. 5. Present $^{13}C(\gamma, p_0)$ (dotted line) and $^{13}C(\gamma, p_1)$ (dashed line) integrated-over-angles cross sections and their sum (dot-dashed line) compared with the $^{13}C(\gamma, p)$ cross section reported in Ref. [3] (small squares with error bars) and that reported by Dennisov, Kulikov, and Kul'chitskii [10], but translated up in energy by 400 keV (solid circles). The results of Patrick et al. [11] are also shown: (γ, p_0) (long-dashed line) and (γ, p_1) (solid line).

not be made, and in the figure it has been extrapolated smoothly down to 21 MeV.

The maximum value of the $^{13}C(\gamma, p_0)$ cross section is approximately 2 mb and occurs near 24.5 MeV, while that of the $^{13}C(\gamma, p_1)$ cross section is approximately 3 mb near 24 MeV. The $^{13}C(\gamma, p_1)$ strength does not fall, and the evidence is that it dominates at high energies. At 26 MeV the p_0 and p_1 channels carry the total strength, and their dominance up to 30 MeV is confirmed by comparison with the measurements of Kosiek et al. [12], and Shin, Wong, and Caplan [13].

The most surprising result in the present work is the observation of a substantial difference between the $^{13}C(\gamma, p)$ and $^{13}C(\gamma, p_0 + p_1)$ cross sections in the GDR region. Most of this excess strength corresponds to the resonance seen in the $^{13}C(\gamma, p)$ cross section near 23.3 MeV. Figure 6 shows the difference between the $^{13}C(\gamma, p)$ and $^{13}C(\gamma, p_0 + p_1)$ cross sections. This excess cross section accounts for about 40% of the $^{13}C(\gamma, p)$ cross section between 21 and 26 MeV, and cannot be accounted for by the experimental uncertainties in either the $^{13}C(\gamma, p)$ cross section from Ref. [3] (±13%) or the present data (∼15%).

This provides the first evidence for population via the photoproton reaction of bound states in ^{12}B other than the ground and first excited states. There are three possible bound states in ^{12}B: at 1.67 (2⁻), 2.62 (1⁻), and 2.72 (0⁺) MeV. Decay of dipole states in ^{13}C to the negative-parity pair is expected to be less likely than decay to the state at 2.72 MeV, since this requires emission of odd-l protons, which can occur only from states with complicated, mixed configurations. This strength is thus identified as due to the $^{13}C(\gamma, p_4)$ channel.

This conclusion is strengthened by data from proton pickup reactions summarized by Ajzenberg-Selove [14] and specifically the work of Pullen et al. [15] and Simmonds et al. [16]. In these studies the 2.72-MeV state in ^{12}B is populated, but not the negative-parity states at 1.67 and 2.62 MeV. The correlation between spectroscopic factors derived from pickup reactions and photoproton decay strength in light nuclei is established by Eramzhyan et al. [17].
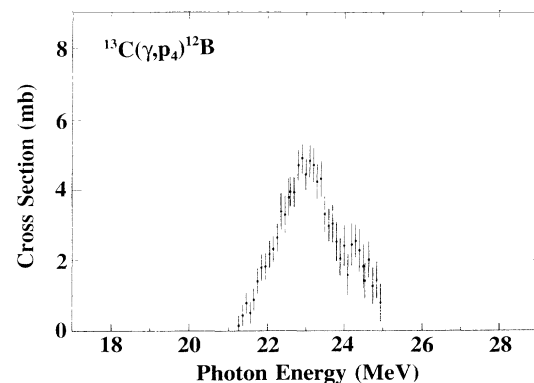
The possibility of any strong decay of the 23-MeV res-

FIG. 6. $^{13}C(\gamma, p_4)$ cross section, obtained by subtracting the reported $^{13}C(\gamma, p_0 + p_1)$ cross sections from the $^3C(\gamma, p)$ cross section reported in Ref. [3].

onance via proton emission to the second excited state can be discounted, since such protons would be above the detection threshold for the present experiment, yet evidence of them is not seen. Furthermore, if this decay occurred, one would expect to see population of the 16.57-MeV analog state in ^{12}C following the ^{13}C(γ, n) reaction. No such strength is seen [18,2].

The predominant decay of the ^{13}C(γ, p) cross section near 23 MeV to the 2.72-MeV state in ^{12}B explains the large discrepancy that has been identified between the cross section as measured using the induced activity and the measurement by direct proton detection: the energies of the protons emitted to the 2.72-MeV state are too low to be detected by the methods used. In addition, the difference in the ^{13}C(γ, p) and ^{13}C(γ, n) cross sections in this energy region is also explained. Since there is little proton decay to the ground and first excited states in ^{12}B, there should be little population of the analog states at 15.11 and 16.11 MeV following neutron emission. The relevant state in ^{12}C [the $T = 1$ analog to the state in ^{12}B that is populated in the ^{13}C(γ, p_4) reaction] is at 17.76 MeV, and the photoneutrons, with an energy of 0.26 MeV, would be strongly suppressed.

The decay preference for the 23-MeV resonance, as discussed above, suggests that it has a significant parentage of a proton coupled to the 0^+ state in ^{12}B state. The ^{13}C ground state, according to Cohen and Kurath [19], contains 72.8% $(1p_{1/2})^1$, 25.6% $(1p_{1/2})^3(1p_{3/2})^{-2}$, and 16% $(1p_{1/2})^4(1p_{3/2})^{-3}$ configurations. The 1^+ and 2^+ states in ^{12}B are strongly dominated by the $(1p_{1/2})^1(1p_{3/2})^{-1}$ configuration and the 0^+ state by the $(1p_{1/2})^2(1p_{3/2})^{-2}$ configuration [20]. Thus the 1^+ and 2^+ states can be formed from the dominant $(1p_{1/2})^1$ component of the ^{13}C ground state by proton transitions from the $1p_{3/2}$ shell to the s-d shell, while the 0^+ state results from transitions to the s-d shell from the $(1p_{1/2})^3(1p_{3/2})^{-2}$ component in the correlated ground state. Consistent with this, it is observed that experimentally proton pickup measurements (see Ref. [14]) populate the 1^+ and 2^+ states by pickup of a $1p_{3/2}$ proton, and the 0^+ state by pickup of a $1p_{1/2}$ proton. Thus the 23-MeV resonance may be considered as a three-particle–two-hole (3p-2h) state relative to the closed ^{12}C core.

Calculations by Höne, Bartz, and Rotter [21] find that 3p-2h configurations account for some 15% of strength in the GDR of ^{13}C and for most of the strength in the high-energy tail. In practice, as reported here, the 3p-2h strength appears to be localized at the state near 23 MeV.

B. Effect of the valence neutron on the core-excited GDR states

In view of the overall aim of the study of which this work forms a part (see Table I of Ref. [22] for a summary), it is worthwhile checking the influence of the valence neutron on the GDR of ^{13}C.

A comparison of the ^{12}C(γ, p_0) cross section compiled by Fuller [23] with the ^{13}C($\gamma, p_0 + p_1$) cross section presented in Fig. 5 shows the effects of the valence neutron

on the major core transition $(1p_{3/2} \to 1d_{5/2})$. No significant change in the width of the GDR of these two nuclei is observed, but the energy of this core transition increases from about 22.8 MeV in ^{12}C to about 24.3 MeV in ^{13}C. Two effects contribute here, isospin splitting and static deformation. The isospin effect lowers the $T_<$ fragment by ~ 2.1 MeV to produce the peak at 20.7 MeV, and increases the main $T_>$ transition (by ~ 1.5 MeV) consistent with the $(2T_0 + 1)$ weighting acting to keep the centroid fixed. The decrease in ground-state deformation of ^{13}C [24] has the effect of increasing the energy of the major transitions.

The similarity of the cross-section structure for the cases of ^{12}C and ^{13}C suggests that J splitting is minimal; it would seem that the interaction of the valence neutron and the core is too weak to separate the multiplets noticeably. A similar situation has been reported for ^{17}O [25].

The peak at 23.3 MeV in the main GDR of ^{13}C, which might suggest multiplet splitting, has been shown above to correspond to a 3p-2h state formed by a proton transition from the $1p_{1/2}$ subshell. It appears to have no counterpart in the ^{12}C cross sections. The absence of a corresponding resonance in the ^{12}C(γ, p_0) cross section is not surprising since it is not seen in the ^{13}C($\gamma, p_0 + p_1$) cross section. However, evidence for it might be expected to be found in the ^{12}C(γ, p) and ^{12}C(γ, n) cross sections.

There is evidence that strength at this same energy exists in the photodisintegration cross section of ^{12}C. The final states populated following the transitions $1p_{1/2} \to 2s$-$1d$ in ^{12}C are the first excited states in ^{11}C and ^{11}B at 2.00 and 2.12 MeV, respectively. Since in this case kinematics do not restrict either the neutron or proton decay to these analog states, the strength should be seen in both proton and neutron decay. Using the compilation of Fuller [23] for the relevant ^{12}C reactions and taking the differences $\sigma(\gamma, p) - \sigma(\gamma p_0)$, and $\sigma(\gamma, n) - \sigma(\gamma, n_0)$, shows strength of about 2 mb in both cases, located near 23 MeV (at the same energy as the main DGR). It is interesting to note that isospin splitting has perturbed the energy of the major transition in ^{12}C, thus revealing this 23-MeV resonance in the case of ^{13}C.

V. CONCLUSIONS

The ^{13}C(γ, p_0) and ^{13}C(γ, p_1) cross sections and angular distributions in the GDR region were derived from a measurement of proton spectra following the ^{13}C(e, p) reaction made at a few angles.

The most important finding in the present work is a strong decay of the GDR at an energy centered about 23 MeV via the ^{13}C(γ, p_4) channel. This previously unreported decay is of comparable magnitude to that to the ground and first excited state. Evidence is presented that this resonance revealed at about 23 MeV is a 3p-2h state formed from the correlated ground state by proton transitions from the $1p_{1/2}$ subshell.

The effect of the valence neutron on the structure and energy distribution of the core-excited states in ^{13}C is

minimal. There is strong similarity in structure observed in the ^{12}C and ^{13}C photonuclear cross sections, suggesting that the interaction between the core and valence neutron is too weak to disrupt the major $E1$ states. The effect of J splitting is not noticeable.

Comparison of the ^{12}C(γ, p_0) and ^{13}C$(\gamma, p_0 + p_1)$ cross sections shows that the $E1$ core transition $(1p_{1/2} \to 1p_{3/2})$ at ~ 22.8 MeV in ^{12}C is split by isospin in ^{13}C to produce the $T_<$ resonance at 20.7 MeV and the major $T_>$ component at ~ 24.3 MeV.

[1] K. G. McNeill, M. N. Thompson, A. D. Bates, J. W. Jury, and B. L. Berman, Phys. Rev. C 47, 1108 (1993).

[2] J. W. Jury, B. L. Berman, D. D. Faul, P. Meyer, K. G. McNeill, and J. G. Woodworth, Phys. Rev. C 19, 1684 (1979).

[3] D. Zubanov, R. A. Sutton, M. N. Thompson, and J. W. Jury, Phys. Rev. C 27, 1957 (1983).

[4] M. Kimura, Y. Torizuka, K. Shoda, M. Sugawara, T. Saito, M. Oyamada, K. Nakahara, K. Itoh, K. Sugiyama, M. Gotoh, K. Miyashita, and K. Kurahashi, Nucl. Instrum. Methods 95, 403 (1971).

[5] C. P. Browne and W. W. Büchner, Rev. Sci. Instrum. 27, 899 (1956).

[6] P. J. Ryan, Ph.D. thesis, University of Melbourne, 1980 (unpublished).

[7] W. C. Barber and T. Wiedling, Nucl. Phys. 18, 575 (1960).

[8] I. C. Nascimento, E. Wolynec, and D. S. Onley, Nucl. Phys. A246, 210 (1975).

[9] l. L. Schiff, Phys. Rev. 83, 252 (1951).

[10] V. P. Denisov, A. V. Kulikov, and L. A. Kul'chitskii, Zh. Eksp. Teor. Fiz. 48, 1488 (1964) [Sov. Phys. JETP 19, 1007 (1964)].

[11] B. H. Patrick, E. M. Bowey, E. J. Winhold, J. M. Reids, and E. G. Muirhead, J. Phys. G 1, 874 (1975).

[12] R. Kosiek, K. Schüpmann, H. W. Siebert, and R. Wendling, Z. Phys. 179, 9 (1964).

[13] Y. M. Shin, C. F. Wong, and H. S. Caplan, Nucl. Phys. A166, 162 (1971).

[14] F. Ajzenberg-Selove, Nucl. Phys. A460, 1 (1986).

[15] D. J. Pullen, A. E. Litherland, S. Hinds, and R. Middleton, Nucl. Phys. 36, 1 (1962).

[16] P. J. Simmonds, K. I. Pierce, P. R. Haynes, N. M. Clarke, R. J. Griffiths, M. C. Mannion, and C. A. Ogalvie, Nucl. Phys. A482, 653 (1988).

[17] R. A. Eramzhyan, B. S. Ishkhanov, I. M. Kapitonov, and V. G. Neudatchin, Phys. Rep. 136, 229 (1986).

[18] R. Koch and H. H. Thies, Nucl. Phys. A272, 296 (1976).

[19] S. Cohen and D. Kurath, Nucl. Phys. 73, 1 (1967).

[20] B. A. Brown, W. E. Ormand, and J. S. Winfield, computer code OXBASH-MSU, the Oxford-Buenos-Aires-Michigan State University, 1986.

[21] J. Höne, H. W. Bartz, and I. Rotter, Nucl. Phys. A330, 109 (1979).

[22] D. J. McLean, M. N. Thompson, D. Zubanov, K. G. McNeill, J. W. Jury, and B. L. Berman, Phys. Rev. C 44, 1137 (1991).

[23] E. G. Fuller, Phys. Rep. 172, 185 (1985).

[24] G. Mairle and G. J. Wagner, Nucl. Phys. A253, 253 (1975).

[25] D. Zubanov, M. N. Thompson, B. L. Berman, J. W. Jury, R. E. Pywell, and K. G. McNeill, Phys. Rev. C 45, 174 (1992).